Optical Materials 53 (2016) 19–23

Contents lists available at ScienceDirect

Optical Materials

journal homepage: www.elsevier.com/locate/optmat

High thermal stability fluorene-based hole-injecting material for organic light-emitting devices

Lu Li, Bo Jiao, Sanfeng Li, Lin Ma, Yue Yu, Zhaoxin Wu *

Key Laboratory of Photonics Technology for Information of Shaanxi Province, Xi'an Jiaotong University, Xi'an 710049, People's Republic of China
Key Laboratory for Physical Electronics and Devices of the Ministry of Education, Xi'an Jiaotong University, Xi'an 710049, People's Republic of China

ARTICLE INFO

Article history:
Received 15 November 2015
Received in revised form 23 December 2015
Accepted 8 January 2016
Available online 12 January 2016

Keywords:
OLED
Hole-injecting materials
Optical properties
Electrical properties
Thermal properties

ABSTRACT

Novel N^1,N^3,N^5-tris(9,9-diphenyl-9H-fluroen-2-yl)-N^1,N^3,N^5-triphenylbenzene-1,3,5-triamine (TFADB) was synthesized and characterized as a hole-injecting material (HIM) for organic light-emitting devices (OLEDs). By incorporating fluorene group TFADB shows a high glass-transition temperature T_g > 168 °C, indicative of excellent thermal stability. TFADB-based devices exhibited the highest performance in terms of the maximum current efficiency (6.0 cd/A), maximum power efficiency (4.0 lm/W), which is improved than that of the standard device based on 4-4′-4″Tris(N-(naphthalene-2-yl)-N-phenyl-amino)triphenylamine (2T-NATA) (5.2 cd/A, 3.6 lm/W). This material could be a promising hole-injecting material, especially for the high temperature applications of OLEDs and other organic electronic devices.

1. Introduction

In recent years, organic light-emitting diodes (OLEDs) have attracted much scientific and commercial interest due to their potential applications in full-color, flat-panel displays and space illumination [1–3]. The past two decades have seen great progress in both device fabrication techniques and materials development [4–7]. For high-performance OLEDs devices, charge injection and transport from both anode and cathode must be balanced off by excitons formed in light emission layer [8,9].

To today, traditional hole injecting materials such as poly(3,4-ethylenedioxythiophene):poly(styrene-4-sulfonate)(PEDOT:PSS) [10–12], 4-4′-4″tris(N-(naphthalene-2-yl)-N-phenyl-amino)triphenylamine (2T-NATA) [13], have been the most widely used because their good performance. However, the thermal stability of these materials do not meet requirement of practical applications. Numerous efforts have been devoted to synthesizing new HIMs with better thermal stability [14].

Fluorene compounds with inherent rigid structures have been attracting attention as organic functional materials because of their special physical and chemical properties, such as high glass transition temperatures, good solubility and their amorphous nature, which make them very promising as an approach for optic electric materials [15,16].

In this work, we designed and synthesized a new compound N^1,N^3,N^5-tris(9,9-diphenyl-9H-fluroen-2-yl)-N^1,N^3,N^5-triphenylbenzene-1,3,5-triamine (TFADB), in which the fluorene moieties were covalently incorporated to the 1,3,5-tris(diphenylamino)benzene (TDAB) core to achieve high-Tg active materials. The compounds were found to form easily stable amorphous films by either vacuum deposition or spin-coating and to function as HIM in OLEDs. The TFADB-based device shows remarkably enhanced performance, over the corresponding 2T-NATA device. The performance of the device indicates that HIM TFADB has potential applications for full-color display.

2. Experimental procedure

The manipulation involving air-sensitive reagents was performed under an inert atmosphere of dry nitrogen. The absorption spectra were obtained using a Hitachi UV 3010 spectrophotometer. The photoluminescence (PL) spectra were collected by a Horiba Jobin Yvon Fluoromax-4 spectrophotometer. Glass transition temperatures (T_g) were determined with a differential scanning calorimeter (DSC, TA instruments DSC200PC) at a heating rate of 10 °C min^{-1} under a N_2 atmosphere. Cyclic voltammetry was performed using a Princeton Applied Research model 273A potentiostat at a scan rate of 100 mV s^{-1}. The HOMO and LUMO values were estimated by using the following general equation:

* Corresponding author at: Key Laboratory of Photonics Technology for Information of Shaanxi Province, Xi'an Jiaotong University, Xi'an 710049, People's Republic of China.
E-mail address: zhaoxinwu@mail.xjtu.edu.cn (Z. Wu).

http://dx.doi.org/10.1016/j.optmat.2016.01.009
0925-3467/

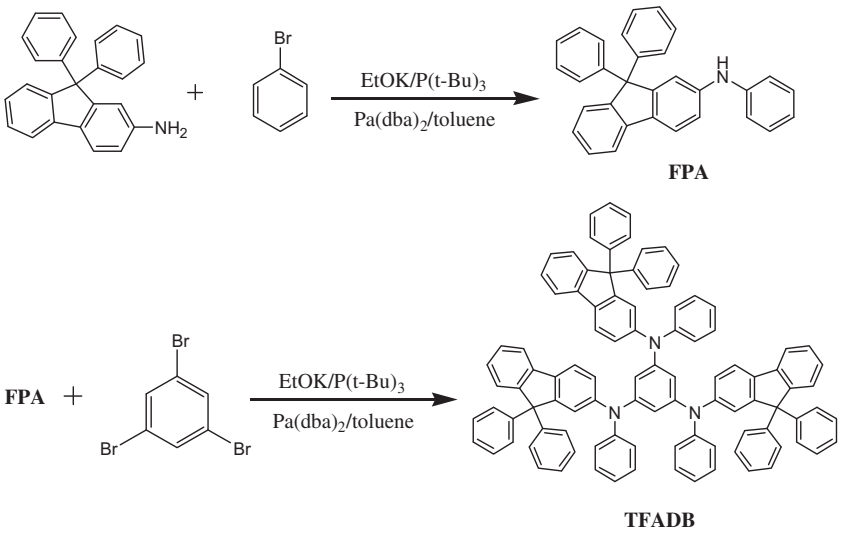

Fig. 1. Synthetic scheme of TFADB.

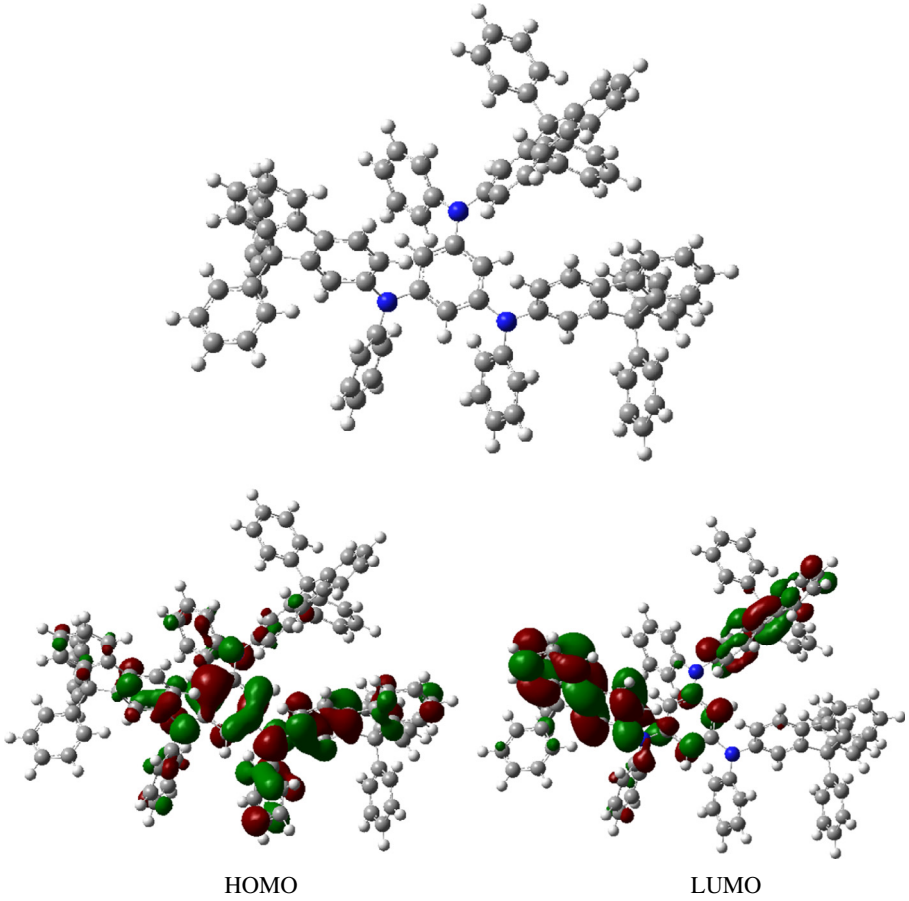

Fig. 2. The optimized geometries and the molecular orbital surfaces of the HOMOs and LUMOs for the TFADB obtained at the B3LYP/6-31G level.

$E_{HOMO} = -(qE_{ox} + 4.8)$ eV; $E_{LUMO} = E_{HOMO} + E_g^{opt}$, which were calculated with the internal standard ferrocene value of −4.8 eV with respect to the vacuum level.

2.1. (9,9-Diphenyl-9H-fluoren-2-yl)-phenyl-amine(FPA)

9,9-Diphenyl-9H-fluoren-2-ylamine (1.8 g, 5.4 mmol), bromobenzene (0.8 g, 5 mmol), potassium t-butoxide (0.84 g, 7.5 mmol), butylphosphine (0.2 ml, 0.01 mmol), tris(dibenzylideneacetone)dipalladium (0.3 g, 0.325 mmol) were added to dry Toluene (30 ml) under nitrogen. The resultant mixture was refluxed for 4 h, quenched using ice-water, extracted with chloroform, and purified by column chromatography with an eluent of ethyl acetate:petrol ether = 1:10. FPA was obtained as a beige solid (1.82 g, 76%). ^{1}H NMR (DMSO, 400 MHz): δ7.26 (m, 4H), 7.56(m, 5H), 7.686–7.874 (m, 8H), 7.94(d, 2H), 8.01(s, 3H). Anal calcd for $C_{31}H_{23}N$: C, 90.95; H, 5.62; N, 3.42. Found: C, 90.91; H, 5.58; N, 3.41.

Table 1
Optical, thermal, and electrochemical properties of the compounds.

Compound	λ_{max}^{Abs} [a] (nm)	λ_{max}^{PLa} (nm)	T_g (°C)	E_{ox} [b] (V)	HOMO/LUMO^{exp} (E_g^{opt}) (eV)	HOMO/LUMO^{cal} ($\Delta E_{HOMO-LUMO}$) (eV)
TFADB	355	410	168	0.42	−5.22/−2.05(3.17)	−5.06/−1.18(3.88)
2-TNATA	325	486	110	0.20	−5.0/−2.1(2.9)	/

[a] Measured in CH_2Cl_2.
[b] Measured versus Fc/Fc+ in CH_2Cl_2.

2.2. N^1,N^3,N^5-tris(9,9-diphenyl-9H-fluroen-2-yl)-N^1,N^3,N^5-triphenyl-benzene-1,3,5-triamine (TFADB)

FPA (1.82 g, 4.4 mmol), 1,3,5-tribromo-benzene (0.44 g, 1.4 mmol), potassium t-butoxide (0.67 g, 6 mmol), butylphosphine (0.2 ml, 0.01 mmol), tris(dibenzylideneacetone)dipalladium (0.28 g, 0.3 mmol) were added to dry Toluene (30 ml) under nitrogen. The resultant mixture was refluxed for 4 h, quenched using ice-water, extracted with chloroform, and purified by column chromatography with an eluent of ethyl acetate:petrol ether = 1:20. TFADB was obtained as a beige solid (0.84 g, 65%). ^{1}H NMR (DMSO, 400 MHz): δ 7.81(d, 3H), 7.79(d, 3H), 7.38(t, 6H), 7.26(t, 3H), 7.23–7.09(m, 24H), 7.01–6.92(d, 18H), 6.90–6.83(m, 9H), 6.14(s, 3H). Anal calcd for $C_{99}H_{69}N_3$: C, 91.45; H, 5.31; N, 3.23. Found: C, 91.43; H, 5.30; N, 3.23.

The hole-injecting layer (HIL), hole-transporting layer (HTL), emitting layer (EML), electron-transporting layer (ETL) and cathode were fabricated by conventional vacuum deposition under a base pressure lower than 1×10^{-3} Pa. The thickness of each layer was determined by a quartz thickness monitor. The effective size of the OLED was 12 mm^2. The OLEDs with the structure of ITO/TFADB or 2T-NATA(50 nm)/NPB (30 nm)/Alq3 (65 nm)/LiF (1 nm)/Al (100 nm) were fabricated. Here, Alq3 (tris(8-hydroxyquinoline) aluminum) served as an electron transporting and light-emitting layer. The voltage–current density (V–J), voltage–brightness (V–L) and current density–current efficiency (J–η) curves of devices were measured with a computer-controlled Keithley 2602 Source-Meter under ambient condition.

3. Results and discussion

Synthetic scheme of TFADB is presented in Fig. 1. TFADB were synthesized by the Ullmann coupling reaction. Theoretical calculations on the electronic states of TFADB were carried out at the DFT//B3LYP/6-31G level in the Gaussian 03 program. As shown in Fig. 2, HOMO are mainly located at central benzene ring and amine groups, then LUMO are mainly located at fluorene groups. The separated HOMO/LUMO can improve carrier transporting. The calculated HOMO and LUMO of TFADB are listed in Table 1.

The thermal properties of TFADB were determined by differential scanning calorimetry (DSC) and shown in Fig. 3 and Table 1. The glass-transition temperature (T_g) of TFADB were determined to be 168 °C, which was high enough as a hole-injecting materials [13]. 9,9-Diphenyl-9H-fluorene with inherent rigid structure leads to this.

The absorption spectra and photoluminescence (PL) spectra of TFADB in CH_2Cl_2 are shown in Fig. 4. The absorption spectra of TFADB in the solution exhibit peaks at 355 nm, respectively, which can be attributed to π–π^* transitions. The solution-PL emission peak occurs at 410 nm. The optical band gaps (E_g) determined from the onset of the absorption spectra are 3.17 eV. TFADB could be applied to HIL due to lake of absorption in visible region of spectrum.

Cyclic voltammetric (CV) studies were performed to calculate the HOMO and LUMO values for the TFADB as shown in Table 1. The HOMO of TFADB is 5.22 eV, which was determined from the anodic oxidation potential by using the previously reported HOMO

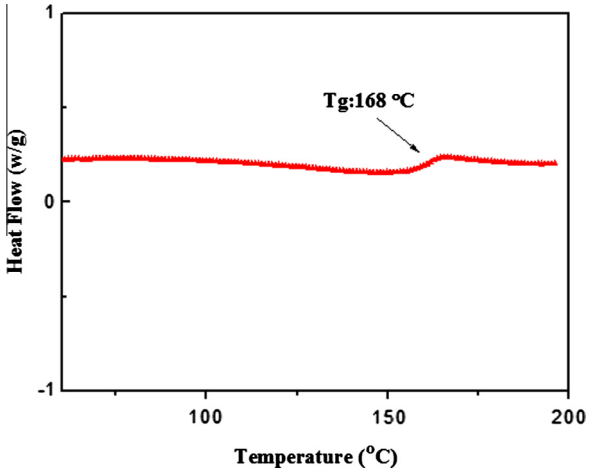

Fig. 3. DSC of TFADB.

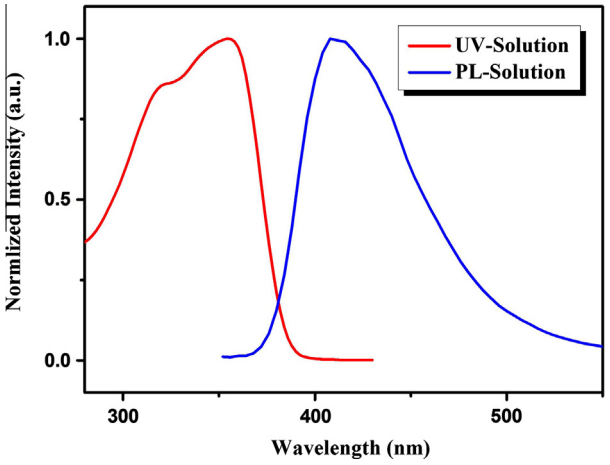

Fig. 4. Absorption and PL spectra of TFADB in CH_2Cl_2.

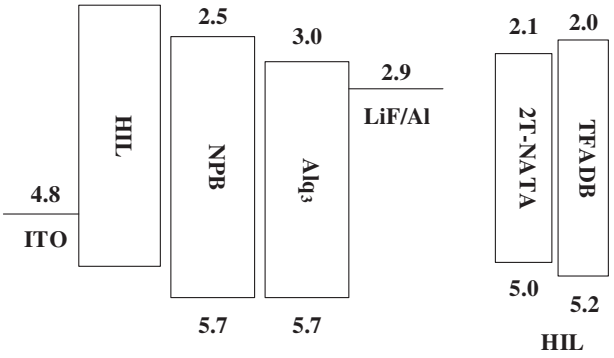

Fig. 5. Energy-level diagram of the devices.

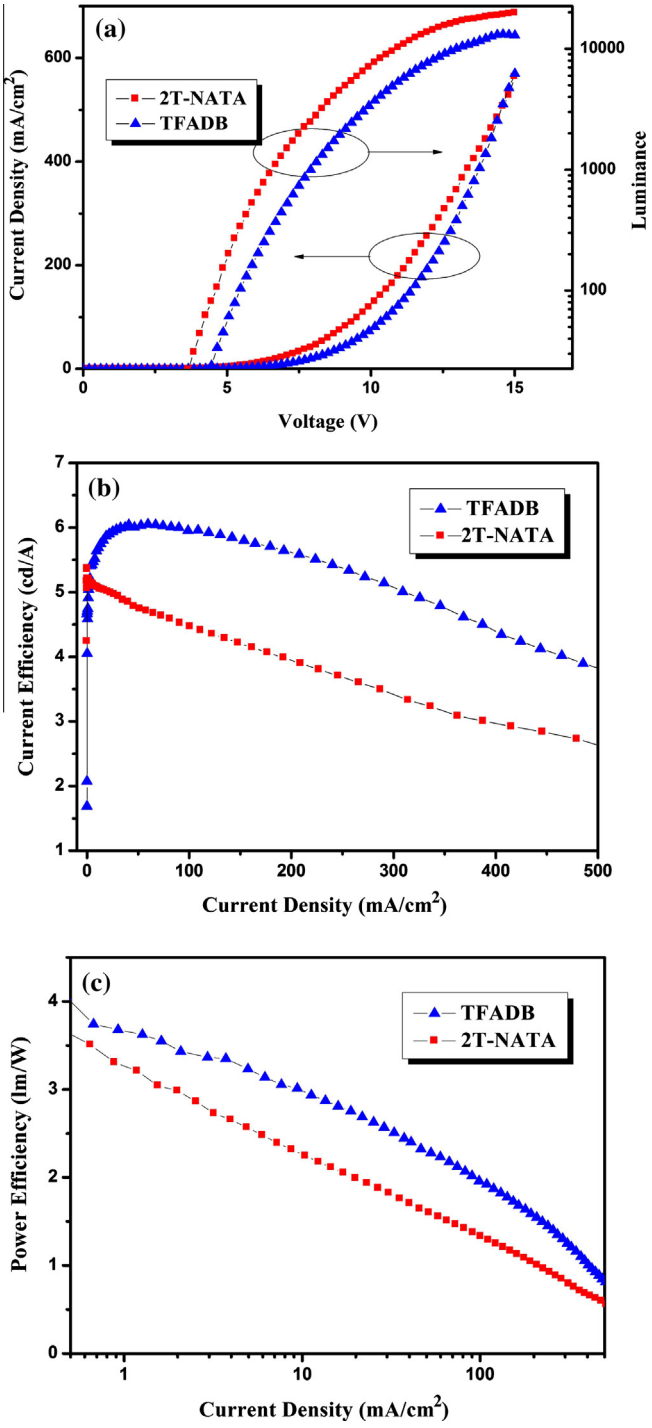

Fig. 6. Current density–luminance–voltage curve (a), current efficiency–current density curves (b), and power efficiency–current density curves (c) for the ITO/2T-NATA or TFADB/NPB/Alq_3/LiF/Al.

of ferrocene (4.8 eV) as a reference. The LUMO was calculated from the HOMO value and the energy gap (E_g) from the edge of the absorption spectrum to be about 2.05 eV, indicating it can block the electrons effectively.

To evaluate the possible applications of TFADB as HIM in OLEDs, we fabricated two devices. The structures of the devices listed below and the energy levels of the materials are shown in Fig. 5 [17].

Device A

ITO/2T-NATA (50 nm)/NPB(30 nm)/Alq_3(65 nm)/LiF(1 nm)/Al (100 nm).

Table 2
Electroluminescent data of the devices.

Devices	V_{on} [a] (V)	L_{max} [b] (cd m^{-2})	η_c [c](cd A^{-1})	η_p [c] (lm/W)
2T-NATA	3.6	25,730	5.2	3.6
TFADB	4.0	20,762	6.0	4.0

[a] Turn-on voltage at 1 cd m^{-2}.
[b] Maximum luminance.
[c] Values collected at a peak efficiency.

Device B

ITO/TFADB (50 nm)/NPB(30 nm)/Alq_3(65 nm)/LiF(1 nm)/Al (100 nm).

The current density–voltage (J–V) characteristics, voltage–luminance (V–L) characteristics, current efficiency–current density (η–J) and power efficiency–current density characteristics are shown in Fig. 6, and the device performances are summarized in Table 2.

As shown in Fig. 6a, at a given voltage, the current density of the TFADB based device is lower than that of the standard device. The current density decrease should be associated with the larger hole injection barrier at the interface between ITO and TFADB. There are two factors affect the driving voltage, namely, energy barrier and tunneling barrier. Considering the HOMO level of TFADB (5.2 eV) is higher than that of 2T-NATA (5.0 eV), the energy barrier should be one reason that increases the driving voltage of TFADB based device. On the other hand, tunneling barrier may be another reason that lower the current density of TFADB based device. The tunneling barrier could influence the charge injection process, and then increases the driving voltage. This could also be supported by the literature reported previously [18–22]. In Fig. 6a, the highest luminance of TFADB and 2T-NATA based devices were 20762 cd/m^2 and 25730 cd/m^2 respectively. Fig. 6b and c shows the current density–current efficiency and current density–power efficiency characteristics for two devices. TFADB-based device exhibits a maximum current efficiency of 6.0 cd/A, which is substantively higher than that of the standard device (5.2 cd/A). Although the TFADB-based device has slightly higher operating voltage than the standard device, the power efficiency of the TFADB-based can reach a valve of 4.0 lm/W, which is higher than that of the standard device (3.6 lm/W). The enhancement in the efficiency of the TFADB-based device can be attributed to the better balanced charge recombination, because the anode, cathode, HTL, ETL, and the emitting layer are the same in both of the TFADB-based device and the standard device.

4. Conclusion

We have designed and synthesized a new amorphous HIM, TFADB. By incorporating fluorene group TFADB shows a high glass-transition temperature T_g > 168 °C, indicative of excellent thermal stability. The TFADB based device showed the current-efficiency of 6.0 cd/A, power efficiency of 4.0 lm/w, which was higher than that of the typical 2T-NATA-based device (5.2 cd/A, 3.6 lm/w). The increased efficiency of the OLEDs with the newly developed HIM is due to the balanced charge recombination in devices, indicated that TFADB could be used a promising hole-injecting material, especially for the high temperature applications of OLEDs and other organic electronic devices.

Acknowledgements

This work was financially supported by Basic Research Program of China (2013CB328705), National Natural Science Foundation of China (Grant Nos. 61275034, 61106123), Ph.D. Programs Founda-

tion of Ministry of Education of China (Grant No. 20130201110065); Fundamental Research Funds for the Central Universities (Grant No. xjj2012087).

References

[1] C.W. Tang, S.A. VanSlyke, Organic electroluminescent diodes, Appl. Phys. Lett. 51 (1997) 913–915.
[2] L.S. Huang, C.H. Chen, Recent progress of molecular organic electroluminescent materials and devices, Mater. Sci. Eng. R 39 (2002) 143–222.
[3] U. Mitschke, P. Bauerle, The electroluminescence of organic materials, J. Mater. Chem. 10 (2000) 1471–1507.
[4] Y. Shirota, Organic materials for electronic and optoelectronic devices, J. Mater. Chem. 10 (2000) 1–25.
[5] Q. Pei, Y. Yang, Efficient photoluminescence and electroluminescence from a soluble polyfluorene, J. Am. Chem. Soc. 118 (1996) 7416–7417.
[6] S.R. Forrest, The road to high efficiency organic light emitting devices, Org. Electron. 4 (2003) 45–48.
[7] P. Strohriegl, J.V. Grazulevicius, Charge-transporting molecular glasses, Adv. Mater. 14 (2002) 1439–1452.
[8] M. Strukelj, M. Papadimitrakopoulos, T.M. Miller, L.J. Rothberg, Design and application of electron-transporting organic materials, Science 267 (1995) 1969–1972.
[9] J.H. Burroughes et al., Light-emitting diodes based on conjugated polymers, Nature 347 (1990) 539–541.
[10] A.C. Arias et al., Organic photodiodes using polymeric anodes, Synth. Met. 102 (1999) 953–954.
[11] W.H. Kim et al., Molecular organic light-emitting diodes using highly conducting polymers as anodes, Appl. Phys. Lett. 80 (2002) 3844–3846.
[12] S. Choulis et al., Interface modification to improve hole-injection properties in organic electronic devices, Adv. Funct. Mater. 16 (2006) 1075–1080.
[13] Y. Shirota, Organic materials for electronic and optoelectronic devices, J. Mater. Chem. C 10 (2000) 1–25.
[14] Y. Shirota, H. Kageyama, Charge carrier transporting molecular materials and their applications in devices, Chem. Rev. 107 (2007) 953–1010.
[15] K. Okumoto, Y. Shirota, Development of new hole-transporting amorphous molecular materials for organic electroluminescent devices and their charge-transport properties, J. Eng. Sci. Technol. B 85 (2001) 135–139.
[16] K. Okumoto, Y. Shirota, A thermally stable greenish blue organic electroluminescent device using a novel emitting amorphous molecular material, Synth. Met. 121 (2001) 1655–1656.
[17] Y. Park, B. Kim, C. Lee, A. Hyun, S. Jang, J.H. Lee, Y.S. Gal, T.H. Kim, K.S. Kim, J. Park, Highly efficient new hole injection materials for OLEDs based on dimeric phenothiazine and phenoxazine derivatives, J. Phys. Chem. C 115 (2011) 4843–4850.
[18] X. Zhou, J. Blochwitz, M. Pfeiffer, A. Nollau, T. Fritz, K. Leo, Enhanced hole injection into amorphous hole-transport layers of organic light-emitting diodes using controlled p-type doping, Adv. Funct. Mater. 11 (2001) 310–314.
[19] C. Ganzorig, M. Fujihira, Improved drive voltages of organic electroluminescent devices with an efficient p-type aromatic diamine hole-injection layer, Appl. Phys. Lett. 77 (2000) 4211–4213.
[20] C.C. Chang, M.T. Hsieh, J.F. Chen, Highly power efficient organic light-emitting diodes with a p-doping layer, Appl. Phys. Lett. 89 (2006) 253504–253507.
[21] S.D. Cai, C.H. Gao, D.Y. Zhou, W. Gu, L.S. Liao, Study of hole-injecting properties in efficient, stable, and simplified phosphorescent organic light-emitting diodes by impedance spectroscopy, Appl. Mater. Interfaces 4 (2012) 312–316.
[22] Z.G. Yin, R. Liu, C. Li, T. Masayuki, C.Z. Liu, X.D. Jin, N1, N1, N3, N3-tetra([1,10-biphenyl]-4-yl)-N5, N5-diphenylbenzene-1,3,5-triamine: synthesis, optical properties and application in OLED devices as efficient hole transporting material, Dyes Pigm. 122 (2015) 59–65.